

Chargino Production and Decay in Photon-Photon-Collisions

T. Mayer¹, H. Fraas²

*Institut für Theoretische Physik, Universität Würzburg,
Am Hubland, D-97074 Würzburg, Germany*

Abstract

We study the production and leptonic decay of charginos in collisions of polarized photon beams including the complete spin correlations. The photons can be generated by Compton backscattering of polarized laser pulses off a polarized electron beam. Since the production process is determined alone by the electromagnetic coupling of the charginos this process allows to study their decay dynamics. The cross section and the forward-backward asymmetry of the decay lepton are very sensitive to the gaugino mass parameter M_1 and to the sneutrino mass without any ambiguities.

Key words:

PACS: 11.30.Pb, 12.60.Jv, 14.80.Ly

1 Introduction

The search for supersymmetric (SUSY) particles and the determination of their properties is one of the main goals of a future e^+e^- Linear Collider in the energy range between 500 GeV and 1000 GeV. Particularly interesting will be the experimental study of charginos. They will be produced with comparably large cross sections and the analysis of their production and decay will allow to measure the parameters of the underlying supersymmetric model. In the Minimal Supersymmetric Standard Model (MSSM) [1] with conserved R parity the chargino masses and couplings are determined by the SUSY parameters M_2 , μ and $\tan \beta$. The neutralino properties and thus the chargino decay

¹ e-mail:mayer@physik.uni-wuerzburg.de

² e-mail:fraas@physik.uni-wuerzburg.de

into the lightest neutralino $\tilde{\chi}_1^0$, which is assumed to be the lightest SUSY particle (LSP), depend in addition on the gaugino mass parameter M_1 . Recently a method has been proposed to separate the chargino production process from the chargino decay and to determine the SUSY parameters M_2 , μ and $\tan\beta$ independently of the neutralino sector [2].

Besides the e^+e^- option also the $\gamma\gamma$ mode of a Linear Collider can be realized with high luminosity polarized photon beams obtained by Compton backscattering of laser pulses off the electron beam. In this contribution we study chargino pair production $\gamma\gamma \rightarrow \tilde{\chi}_i^+ \tilde{\chi}_i^-$ ($i = 1, 2$) and for the case of the lighter charginos the subsequent leptonic decay $\tilde{\chi}_1^+ \rightarrow \tilde{\chi}_1^0 e^+ \nu_e$. The chargino exchange in the t- and u-channel of the production process is determined by the electromagnetic coupling of the chargino and, apart from the chargino mass, completely independent of the SUSY parameters. Therefore the combined process of production and decay allows to study the decay mechanism separated from the model independent production mechanism. The unpolarized production cross section for the charginos is not suppressed by destructive interference effects [3] and larger than for chargino production in e^+e^- annihilation by a factor of 2.4 at $\sqrt{s} = 500$ GeV and even by a factor of 9 at $\sqrt{s} = 1000$ GeV. By appropriate choice of the polarization of the photon beams it can be enhanced. As a further advantage the polarization of the chargino is solely determined by the polarization of the photon beams and can be modified by changing the polarization of the laser beam and the converted electron beam.

2 Cross Sections and Decay Angular Distributions

The helicity amplitudes for the pure electromagnetic production process $\gamma(\alpha)\gamma(\beta) \rightarrow \tilde{\chi}_i^+(\lambda_i)\tilde{\chi}_i^-(\lambda_j)$ proceeding via chargino exchange in the t- and u-channel are denoted by $T_{P,\alpha\beta}^{\lambda_i\lambda_j}$. Here α, β are the helicities of the photons and λ_i, λ_j the helicities of the charginos. The direct leptonic decay $\tilde{\chi}_i^\pm \rightarrow \tilde{\chi}_1^0 e^\pm \nu_e^{(\mp)}$ proceeds via W^\pm, \tilde{e}_L and $\tilde{\nu}_e$ exchange with helicity amplitudes $T_D^{\lambda_i} (T_D^{\lambda_j})$. The amplitude squared of the combined process of production and decay is (summed over chargino helicities)

$$|T_{\alpha\beta}|^2 = |\Delta(\tilde{\chi}_i^+)|^2 |\Delta(\tilde{\chi}_i^-)|^2 \rho_{P,\alpha\beta}^{\lambda_i\lambda_j, \lambda'_i\lambda'_j} \rho_D^{\lambda'_i\lambda_i} \rho_D^{\lambda'_j\lambda_j}. \quad (1)$$

It is composed of the (unnormalized) spin density production matrix

$$\rho_{P,\alpha\beta}^{\lambda_i\lambda_j, \lambda'_i\lambda'_j} = T_{P,\alpha\beta}^{\lambda_i\lambda_j} T_{P,\alpha\beta}^{\lambda'_i\lambda'_j*}, \quad (2)$$

which is, apart from the chargino mass, independent of the SUSY parameters, the decay matrices

$$\rho_D^{\lambda'_i \lambda_i} = T_D^{\lambda_i} T_D^{\lambda'_i *} \quad \rho_D^{\lambda'_j \lambda_j} = T_D^{\lambda_j} T_D^{\lambda'_j *} \quad (3)$$

and the propagator $\Delta(\tilde{\chi}_i) = \frac{1}{p_i^2 - m_i^2 + im_i \Gamma_i}$. Here p_i^2, m_i and Γ_i are the four-momentum squared, mass and width of $\tilde{\chi}_i^\pm$. For this propagator we use the narrow width approximation. For further details of this spin formalism including full spin correlations between production and decay see [4,5]. The production density matrix $\rho_{P,\alpha\beta}^{\lambda_i \lambda_j, \lambda'_i \lambda'_j}$ for polarized photons will be given in a forthcoming paper. The decay density matrix can be found in [4]. The photon beams are produced by Compton backscattering of circularly polarized laser photons off longitudinal polarized electrons. The energy spectrum and the mean helicity of the high energy photons sensitively depend on the polarization of the laser photons and of the converted electrons and are given in [6]. To obtain the cross sections and the angular distributions of the decay electrons in the laboratory frame (ee-cms) one has to convolute the cross section in the $\gamma\gamma$ -cms with the energy distribution and the mean helicity of the backscattered photon beams [7,8]. In the next section we give numerical results for the production and subsequent leptonic decay $\tilde{\chi}_1^+ \rightarrow \tilde{\chi}_1^0 e^+ \nu_e$ of the lighter chargino and for the forward-backward asymmetry

$$A_{\text{FB}} = \frac{\sigma(\cos \theta > 0) - \sigma(\cos \theta < 0)}{\sigma(\cos \theta > 0) + \sigma(\cos \theta < 0)} \quad (4)$$

of the decay positron in the laboratory frame. In equ. (4) θ describes the angle between the decay positron and the converted electron beam.

3 Numerical Results

For the numerical analysis we fix the MSSM parameters

$$M_2 = 152 \text{ GeV}, \quad \mu = 316 \text{ GeV}, \quad \tan \beta = 3, \quad (5)$$

which lead to a gaugino-like lightest chargino $\tilde{\chi}_1^\pm$ with the mass $m_{\tilde{\chi}_1^\pm} = 128 \text{ GeV}$.

In fig. 1 we show the energy dependence of the production cross section $\sigma_p(e^+e^- \rightarrow \tilde{\chi}_1^+ \tilde{\chi}_1^-)$ for different polarization configurations. The optimal polarization configuration depends on the beam energy. For $\sqrt{s_{ee}} = 500 \text{ GeV}$ one obtains the highest cross section for $(\lambda_{k_1}, \lambda_{L_1}) = (1, 0)$ and $(\lambda_{k_2}, \lambda_{L_2}) = (1, 0)$,

whereas for $\sqrt{s_{ee}} > 800$ GeV the configuration $(\lambda_{k_1}, \lambda_{L_1}) = (1, 0)$, $(\lambda_{k_2}, \lambda_{L_2}) = (-1, 0)$ is favoured.

In fig. 2 the angular distribution of the positron from the leptonic decay $\tilde{\chi}_1^+ \rightarrow \tilde{\chi}_1^0 e^+ \nu_e$ is depicted for $\sqrt{s_{ee}} = 500$ GeV. It additionally depends on the SUSY parameter M_1 and on the masses of the sneutrino and the left selectron. As an example we have chosen $m_{\tilde{\nu}_e} = 234$ GeV and $M_1 = 78.7$ GeV according to the GUT relation $M_1 = \frac{5}{3} \tan^2 \theta_W M_2$. This corresponds to the DESY/ECFA reference scenario for the Linear Collider [9]. The mass of the left selectron is determined by the $SU(2)_L$ relation [10]

$$m_{\tilde{e}_L}^2 = m_{\tilde{\nu}_e}^2 - m_W^2 \cos 2\beta. \quad (6)$$

For the polarization configuration $(\lambda_{k_1}, \lambda_{L_1}) = (1, 0)$, $(\lambda_{k_2}, \lambda_{L_2}) = (1, 0)$ the positron angular distribution is forward-backward symmetric, whereas for $(\lambda_{k_1}, \lambda_{L_1}) = (1, 0)$ and $(\lambda_{k_2}, \lambda_{L_2}) = (-1, 0)$ the backward direction is preferred with a rather large asymmetry $A_{FB} = -11.6\%$. Unpolarized beams lead to a vanishing forward-backward asymmetry.

Fig. 3 shows for $\sqrt{s_{ee}} = 500$ GeV and $M_1 = 78.7$ GeV the $m_{\tilde{\nu}_e}$ dependence of the cross section $\sigma = \sigma_p \times BR(\tilde{\chi}_1^+ \rightarrow \tilde{\chi}_1^0 e^+ \nu_e)$ for beam polarizations $(\lambda_{k_1}, \lambda_{L_1}) = (1, 0)$ and $(\lambda_{k_2}, \lambda_{L_2}) = (-1, 0)$. Since the chargino production cross section σ_p is independent of the SUSY parameters fig. 3 reflects the $m_{\tilde{\nu}_e}$ dependence of the leptonic branching ratio. The selectron mass is chosen according to equ. (6). Fig. 4 shows the corresponding forward-backward asymmetry of the decay positron. For $m_{\tilde{\nu}_e} < 250$ GeV the cross section shows a significant $m_{\tilde{\nu}_e}$ dependence whereas A_{FB} is sensitive to the sneutrino mass up to $m_{\tilde{\nu}_e} \sim 400$ GeV. Since neither the cross section nor A_{FB} show ambiguities this process should allow to determine the sneutrino mass in the region $m_{\tilde{\nu}_e} \lesssim 400$ GeV. With increasing $m_{\tilde{\nu}_e}$ the contributions from $\tilde{\nu}_e$ and \tilde{e}_L exchange to the chargino decay are more and more suppressed so that finally only the contribution from W exchange survives.

Finally we give up the GUT-relation between M_1 and M_2 and show for $\sqrt{s_{ee}} = 500$ GeV in figs. 5 and 6, respectively, the cross section and A_{FB} as a function of the gaugino mass parameter M_1 in the region $40 \text{ GeV} < M_1 < 280$ GeV. The beam polarizations are again $(\lambda_{k_1}, \lambda_{L_1}) = (1, 0)$ and $(\lambda_{k_2}, \lambda_{L_2}) = (-1, 0)$. For the sneutrino mass we have chosen $m_{\tilde{\nu}_e} = 234$ GeV and the selectron mass is $m_{\tilde{e}_L} = 245$ GeV, corresponding to equ. (6). The decay $\tilde{\chi}_1^+ \rightarrow \tilde{\chi}_1^0 e^+ \nu_e$ proceeds via \tilde{e}_L , $\tilde{\nu}_e$ and W exchange so that the M_1 dependence of the cross section and of A_{FB} is determined by the interplay between the M_1 dependence of the LSP mass and the M_1 dependence and the relative magnitude of the relevant couplings. Similar as for the $m_{\tilde{\nu}_e}$ dependence the M_1 dependence of the cross section reflects that of the leptonic branching ratio of the chargino decay. For large M_1 the mass of the LSP and the couplings are nearly independent of

M_1 [11], leading to the flat run of the cross section and the forward-backward asymmetry. Between $M_1 = 50$ GeV and $M_1 = 100$ GeV the cross section increases approximately 10% and for $M_1 > 100$ GeV it is nearly independent of M_1 . The forward-backward asymmetry, however, shows a pronounced M_1 -dependence between $M_1 = 50$ GeV and $M_1 = 150$ GeV. Since there are no ambiguities it should be possible to determine M_1 in this region from a measurement of the forward-backward asymmetry.

4 Conclusion

We have studied the production of charginos at a 500 GeV Linear Collider in the $\gamma\gamma$ mode including the complete spin correlations between production and the subsequent leptonic decay. For $m_{\tilde{\nu}_e} < 250$ the cross section is strongly dependent on $m_{\tilde{\nu}_e}$. The forward-backward asymmetry of the decay leptons shows a pronounced dependence on the gaugino mass parameter M_1 in the region $50 \text{ GeV} < M_1 < 150 \text{ GeV}$ and on the sneutrino mass for $m_{\tilde{\nu}_e} \lesssim 400$ GeV. Since neither the M_1 dependence nor the $m_{\tilde{\nu}_e}$ dependence of the cross section and the asymmetry show ambiguities, this process should allow to test the GUT relation between M_1 and M_2 and to determine the sneutrino mass.

Acknowledgements

We are grateful to Gudi Moortgat-Pick and Claus Blöchliger for numerous valuable discussions. We also thank Fabian Franke for many helpful comments on the manuscript. This work was supported by the Deutsche Forschungsgemeinschaft under contract no. FR 1064/4-1 and the Bundesministerium für Bildung und Forschung (BMBF) under contract no. 05 HT9WWA 9.

References

- [1] H. E. Haber, G. L. Kane, *Phys. Rep.* 117 (1985) 75.
- [2] S. Y. Choi, A. Djouadi, H. S. Song, P. M. Zerwas, *Eur. Phys. J. C* 8 (1999) 669.
- [3] A. Bartl, H. Fraas, W. Majerotto, B. Mösslacher, *Z. Phys.* C55 (1992) 257.
- [4] G. Moortgat-Pick, H. Fraas, A. Bartl, W. Majerotto, *Eur. Phys. J. C* 7 (1998) 113.
- [5] G. Moortgat-Pick, H. Fraas, A. Bartl, W. Majerotto, *Eur. Phys. J. C* 9 (1999) 521.

- [6] I. F. Ginzburg, G. L. Kotkin, S. L. Panfil, V. G. Serbo, V. I. Telnov, *Nucl. Inst.* 219 (1984) 5.
- [7] T. Kon, K. Nakamura, T. Kobayashi, *Z. Phys.* C45 (1990) 567.
- [8] S. Hesselbach, H. Fraas, *Phys. Rev. D* 55 (1997) 1343.
- [9] S. Ambrosanio, G. A. Blair, P. Zerwas, ECFA-DESY LC-Workshop, 1998.
- [10] S. P. Martin, P. Raymond, *Phys. Rev. D* 48 (1993) 5365.
- [11] C. Blöchliger, H. Fraas, hep-ph/0001034.

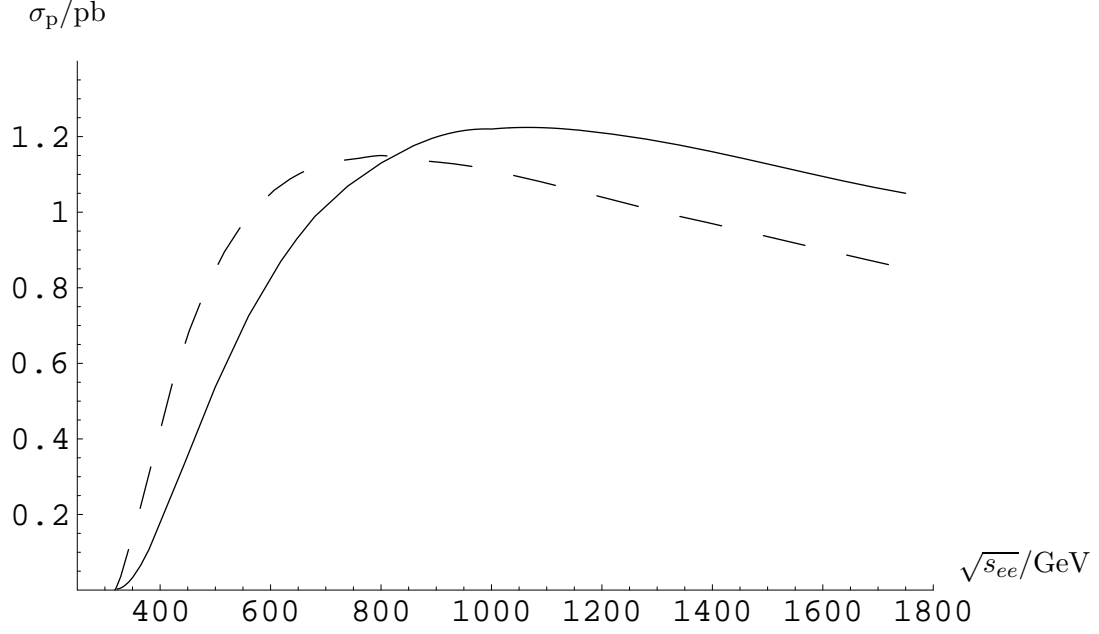


Fig. 1. Production cross section $\sigma_p(\gamma\gamma \rightarrow \tilde{\chi}_1^+ \tilde{\chi}_1^-)$ as a function of the cms energy for $m_{\tilde{\chi}_1^\pm} = 128$ GeV, $(\lambda_{k_1}, \lambda_{L_1}) = (1, 0)$, $(\lambda_{k_2}, \lambda_{L_2}) = (1, 0)$ (dashed line) and $(\lambda_{k_1}, \lambda_{L_1}) = (1, 0)$, $(\lambda_{k_2}, \lambda_{L_2}) = (-1, 0)$ (solid line).

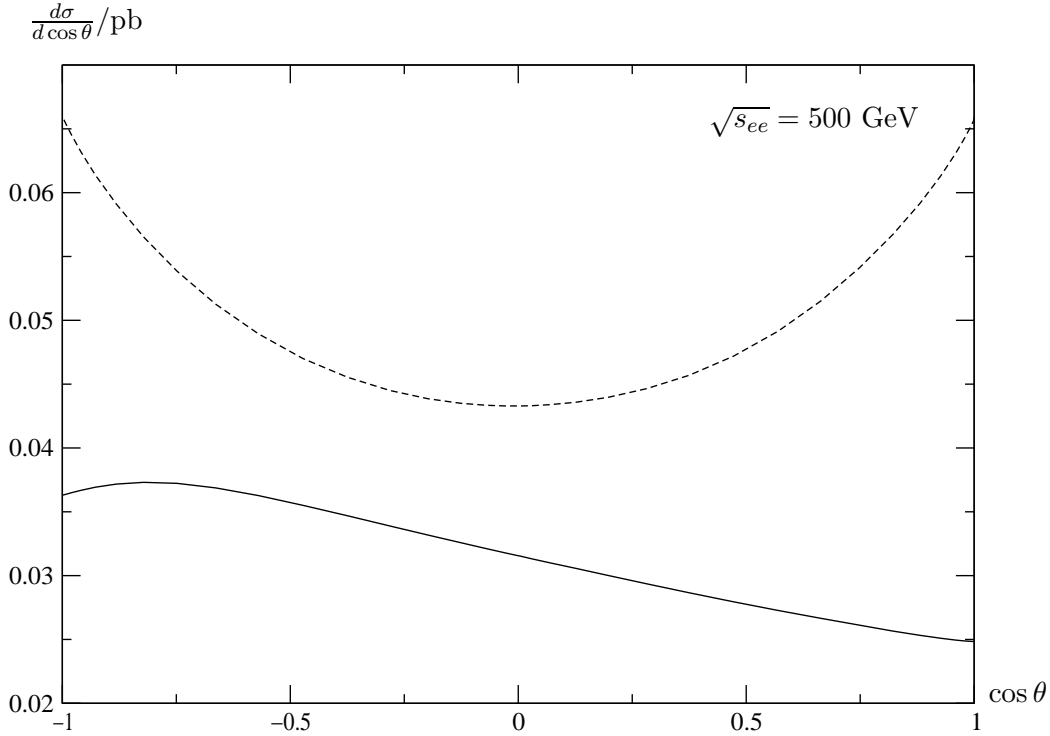


Fig. 2. Angular distribution of the decay positron in $\gamma\gamma \rightarrow \tilde{\chi}_1^+ \tilde{\chi}_1^-$, $\tilde{\chi}_1^+ \rightarrow \tilde{\chi}_1^0 e^+ \nu_e$ at $\sqrt{s_{ee}} = 500$ GeV for $m_{\tilde{\nu}_e} = 234$ GeV, $M_1 = 78.8$ GeV, $(\lambda_{k_1}, \lambda_{L_1}) = (1, 0)$, $(\lambda_{k_2}, \lambda_{L_2}) = (1, 0)$ (dashed line) and $(\lambda_{k_1}, \lambda_{L_1}) = (1, 0)$, $(\lambda_{k_2}, \lambda_{L_2}) = (-1, 0)$ (solid line).

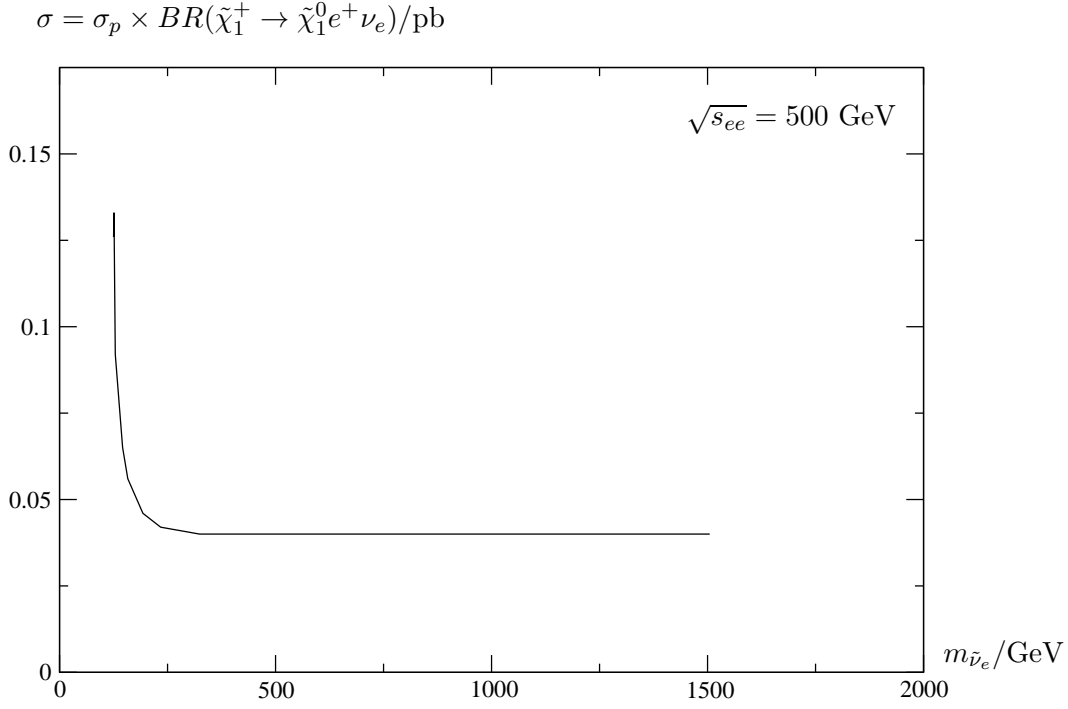


Fig. 3. Cross section for $\gamma\gamma \rightarrow \tilde{\chi}_1^+ \tilde{\chi}_1^-$, $\tilde{\chi}_1^+ \rightarrow \tilde{\chi}_1^0 e^+ \nu_e$ as a function of the sneutrino mass at $\sqrt{s_{ee}} = 500 \text{ GeV}$ for $M_1 = 78.7 \text{ GeV}$, $(\lambda_{k_1}, \lambda_{L_1}) = (1, 0)$ and $(\lambda_{k_2}, \lambda_{L_2}) = (-1, 0)$.

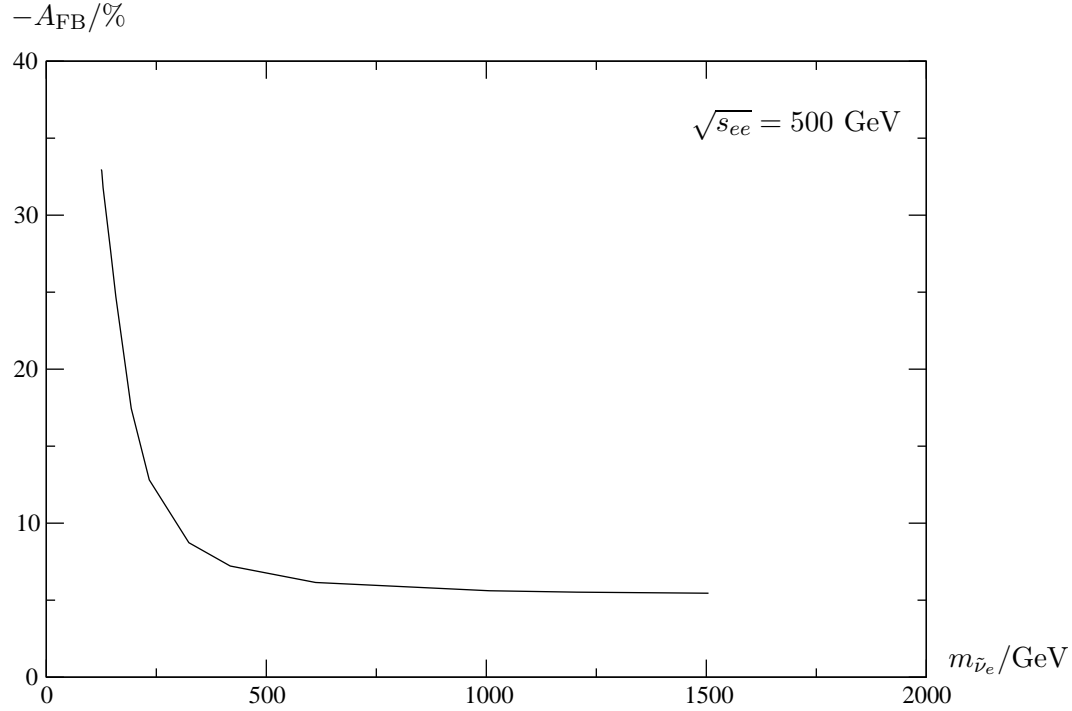


Fig. 4. Forward-Backward asymmetry for $\gamma\gamma \rightarrow \tilde{\chi}_1^+ \tilde{\chi}_1^-$, $\tilde{\chi}_1^+ \rightarrow \tilde{\chi}_1^0 e^+ \nu_e$ as a function of the sneutrino mass at $\sqrt{s_{ee}} = 500 \text{ GeV}$ for $M_1 = 78.7 \text{ GeV}$, $(\lambda_{k_1}, \lambda_{L_1}) = (1, 0)$ and $(\lambda_{k_2}, \lambda_{L_2}) = (-1, 0)$.

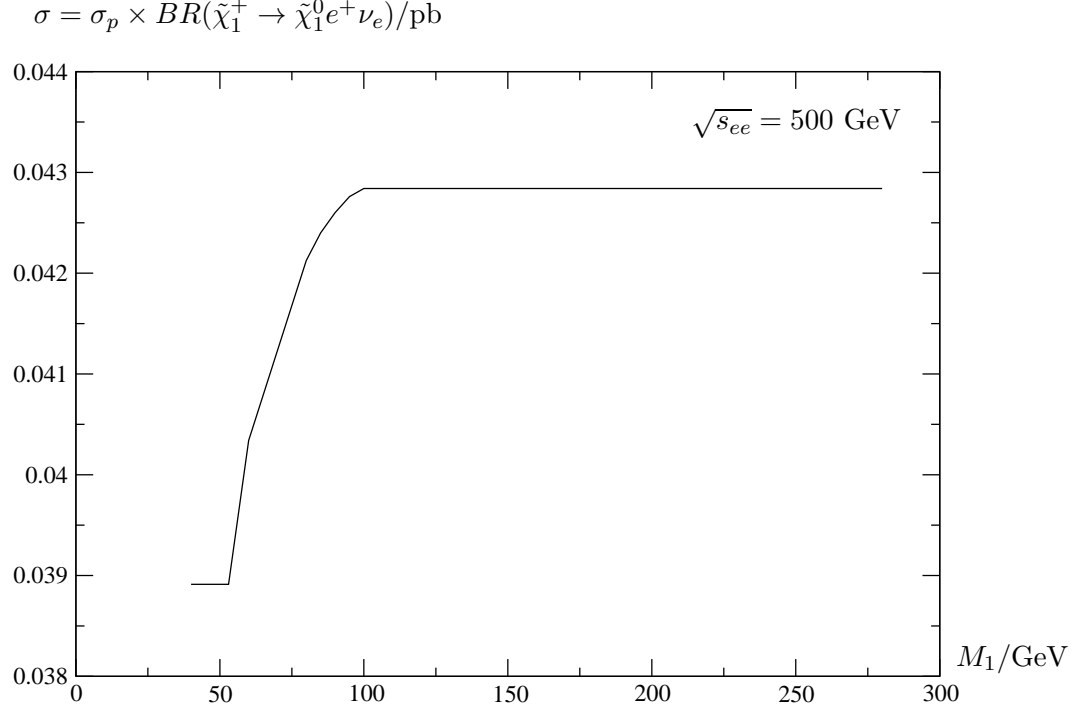


Fig. 5. Cross section for $\gamma\gamma \rightarrow \tilde{\chi}_1^+ \tilde{\chi}_1^-$, $\tilde{\chi}_1^+ \rightarrow \tilde{\chi}_1^0 e^+ \nu_e$ as a function of the parameter M_1 at $\sqrt{s_{ee}} = 500 \text{ GeV}$ for $m_{\tilde{\nu}_e} = 234 \text{ GeV}$, $(\lambda_{k_1}, \lambda_{L_1}) = (1, 0)$ and $(\lambda_{k_2}, \lambda_{L_2}) = (-1, 0)$.

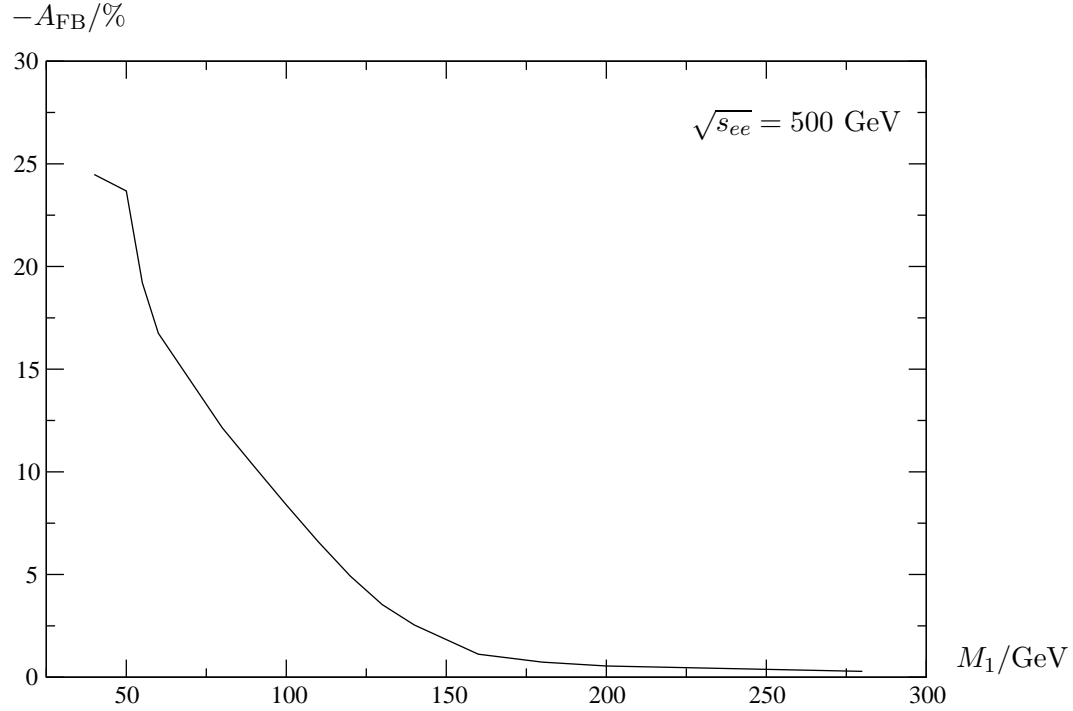


Fig. 6. Forward-Backward asymmetry for $\gamma\gamma \rightarrow \tilde{\chi}_1^+ \tilde{\chi}_1^-$, $\tilde{\chi}_1^+ \rightarrow \tilde{\chi}_1^0 e^+ \nu_e$ as a function of the parameter M_1 at $\sqrt{s_{ee}} = 500 \text{ GeV}$ for $m_{\tilde{\nu}_e} = 234 \text{ GeV}$, $(\lambda_{k_1}, \lambda_{L_1}) = (1, 0)$ and $(\lambda_{k_2}, \lambda_{L_2}) = (-1, 0)$.